A starting from zero DC voltage build-up procedure for a magnet-free synchronous reluctance generator in reduced speed operation

Laurent Schuller, Jean-Yves Gauthier, Romain Delpoux, Xavier Brun

ELECTRIMACS 2022 – Nancy, France, 16th-19th May 2022

A starting from zero DC voltage build-up procedure for a magnet-free synchronous reluctance generator in reduced speed operation

Laurent Schuller · Jean-Yves Gauthier · Romain Delpoux · Xavier Brun

Abstract This paper proposes a parametrized procedure for the voltage build-up of a synchronous reluctance generator connected to a three-phase, two-level controlled rectifier. The magnet-free synchronous reluctance generator is considered in severe conditions where it is neither connected to the grid nor to an electrical energy storage system. Moreover, a reduced speed operation is assumed. The procedure is based on an analysis of the torque generated by the interaction between the residual magnetism and the currents of the generator that maximize the reluctant torque. The choice of the procedure's parameters that improve the chances of successful voltage build-up are discussed. Experimental verifications are carried out in order to illustrate the analysis.

1 Introduction

Today's economical and ecological issues force the machine constructors to use less rare-earth magnets [3]. Thus, the machine technologies with no magnet such as the synchronous reluctance machine (SynRM) gained a lot of interest since a few years [8]. Thanks to this enthusiasm, the advances in the power electronics and the development of novel designs [11] for SynRM, this type of machine challenges nowadays the traditional induction machine (IM) [2]. In particular, the better efficiency and the lower weight of the SynRM compared to the IM [12] makes this technology viable for electrical vehicle application [1, 15]. However as the IM, the lack of magnet in the rotor of the SynRM complicates its use as a generator. Indeed, these generators must be magnetised in order to recover power. Using an IM or a SynRM as a generator when no electrical supply is available is a challenging task.

This kind of operation is based on the so called self excitation phenomenon and has already been studied firstly for yhe induction generator [4,16] and then for the synchronous reluctance generator (SynRG) [7, 10, 18]. Concerning the self excited SynRG, in [7, 10, 18] the authors focused on a three-phase voltage generation. This operation does not employ a power converter, thus neither a control algorithm. In addition, the system requires a three-phase capacitor bank, called excitation capacitors, in order to start the generator. The produced three-phase voltage then depends on the speed of the rotor, the capacitors values and the load. A controlled voltage build-up of an induction generator has been proposed in [9] where a three-phase excitation capacitor bank is used and a single stage DC converter is connected to the generator. In [5,6], the authors successfully build-up the DC voltage of an induction generator when it was running in over speed operation. In such conditions, the controlled voltage build-up starts with a substantial voltage at the DC capacitor terminals.

For all the mentioned studies, the residual magnetism of the machine has been identified as a crucial phenomenon to ensure the voltage build-up of the generator. The modelling of the back electromotive forces (EMF) due to the residual magnetism in the SynRM has been the subject of a previous study [14]. The on-line determination of these back EMF has been proposed in [13].

In this paper, the authors propose a description of the torque generated during the voltage build-up of a SynRG. The effect of the residual magnetism is taken into account and its impact is discussed. During the beginning of the voltage build-up, both EMF and reluctant part of the torque must be considered. Based on the above, a procedure that includes the choice of the magnetization of the machine is proposed to facilitate the voltage build-up of a SynRG. This proce-

L. Schuller · J-Y. Gauthier · R. Delpoux · X. brun
Laboratoire Ampère – INSA de Lyon
25 Avenue Jean Capelle 69100 Villeurbanne cedex, France
e-mail: laurent.schuller@insa-lyon.fr, jean-yves.gauthier@insa-lyon.fr, romain.delpoux@insa-lyon.fr, xavier.brun@insa-lyon.fr

dure would be useful for generating a constant voltage in a remote area through a mechanical power generator as a wind turbine for example. This strategy does not require a three-phase capacitor bank neither a preloaded capacitor on the DC side.

The paper is structured as follows: the considered system is presented and its modelling is given in section 2. The effect of the residual magnetism on the torque is discussed in section 3. In section 4, the proposed voltage build-up strategy is developed. In section 5, the experimental voltage build-up results are shown and discussed. Finally the conclusion and the future works are given in section 6.

2 Presentation of the system

2.1 Global view of the system

Fig.1 shows the system considered in this work. This system is proposed for a stand alone electrical power generator. A prime mover (such as a wind turbine or a tidal turbine) drives the SynRG at constant mechanical speed Ω. The SynRG is connected to a single stage power converter. The power converter is a three-phase two-level active rectifier with a capacitor on its DC side. In addition to smoothing the voltage, the capacitor is a small energy storage that is assumed to be initially discharged. The purpose of this system is to feed a DC load with a regulated DC voltage. The DC load is initially disconnected (*Sw* open) and is connected by closing the switch *Sw* when the DC voltage reached its desired value.

The losses of the converter are modelled by a resistor R_c [19] whose value is unknown and depends on the operating point. Although the active rectifier makes the system more complex, it allows to control the voltage build-up and to regulate v_{dc} even under speed or load changes. During the voltage build-up, the load is considered constant and equal to R_L^0. This resistance is placed in parallel with the capacitor for safety reasons. The capacitor can discharge in the resistance R_L^0 when the system is shut down. In the rest of the paper, the total resistive load $R_L = R_L^0 // R_c$ is often considered. The objective of the proposed strategy is to ensure the so called voltage build-up that corresponds to the increase of the DC voltage.

2.2 Modelling of the system

The electrical behaviour of the SynRM in the Park reference frame (the "*d*" axis is aligned with the low reluctance direction) is modelled by the equations (1a). The quantities e_d and e_q account for the back EMF due to the residual magnetism within the machine [14].

$$\begin{aligned} L_d \frac{di_d}{dt} &= v_d - R_s i_d + n_{pp}\Omega L_q i_q - e_d, \\ L_q \frac{di_q}{dt} &= v_q - R_s i_q - n_{pp}\Omega L_d i_d - e_q, \end{aligned} \tag{1a}$$

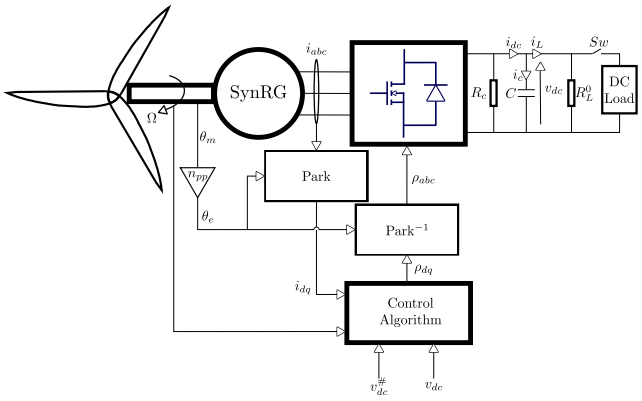

Fig. 1 Representation of the considered system

$$\begin{aligned} e_d &= -n_{pp}\Omega\sqrt{\frac{3}{2}}\left(e_0 sin(\delta_0) + e_2 sin(n_{pp}\theta_m - \sigma_0)\right), \\ e_q &= n_{pp}\Omega\sqrt{\frac{3}{2}}\left(e_0 cos(\delta_0) + e_2 cos(n_{pp}\theta_m - \sigma_0)\right). \end{aligned} \tag{1b}$$

The variables i_d, i_q and v_d, v_q are respectively the currents and the voltages in the direct and quadrature axis of the Park reference frame. The parameters e_0 and δ_0 are constants. The parameter e_2 is constant and represents the amplitude of the back EMF's frequency components, σ_0 is its phase shift. The electrical parameters R_s, L_d and L_q are respectively the phase resistor, the direct inductance and the quadratic inductance of the machine, they are considered constant in this work. The mechanical position and speed of the machine are θ_m and Ω respectively . The number of pole pairs of the SynRM is noted n_{pp}.

The DC voltage dynamic can be determined by a power balance. The Park transform considered conserves the amplitude but not the power. This leads to the equation (2).

$$-C\frac{dv_{dc}}{dt} = \frac{3}{2}\left(\rho_d i_d + \rho_q i_q\right) + \frac{1}{R_L}v_{dc} + i_{Load}, \tag{2}$$

where ρ_d, ρ_q are the duty cycles in the Park reference frame.The current i_{Load} is the current flowing through the DC Load and is zero when the switch *Sw* is open. The voltages v_d and v_q are linked to the duty cycles ρ_d and ρ_q by the relations $v_d = \rho_d v_{dc}$ and $v_q = \rho_q v_{dc}$.

To increase the voltage v_{dc}, the power recovery of the system must increase, at constant speed this is equivalent to raise the torque of the SynRG in opposition with its speed. When the back EMF are considered, the torque produced by the SynRG is expressed in (3).

$$\Gamma_{em} = n_{pp}\frac{3}{2}(L_d - L_q)i_d i_q + \frac{1}{\Omega}\frac{3}{2}\left(e_d i_d + e_q i_q\right). \tag{3}$$

In this work, the first term on the right hand side of (3) is referred as reluctant torque and the second one is called EMF torque.

Remark 1 Because the back EMF e_d and e_q are proportional to the speed, the EMF torque does not depend on the speed value.

Generally speaking, the reluctant torque is paramount over the EMF torque. However, depending on the current level $I = \sqrt{i_d^2 + i_q^2}$, the EMF torque can be more important than the reluctant torque. This is particularly true at low current level, indeed, a linearisation around $i_d = i_q = 0A$ shows that the reluctant torque is negligible in such operation. Moreover, it is known that the SynRM has a low saliency level at low current because the iron ribs on the "q" axis are not saturated [17]. In other words, the EMF torque is preponderant for small amounts of current whereas the reluctant torque becomes dominant when I increases. Finding a global solution for the current repartition that maximizes the average value of the total torque and that takes into account the magnetic saturations, the back EMF and their potential changes is a very challenging task. In order to simplify this issue, in this paper, we consider the classical control $i_d = \pm i_q$ case with constant inductances. Throughout the rest of this study, we consider a positive speed for the generator, the generalization of the reasoning for a negative speed is quite simple.

3 Average torque analysis with $\Omega > 0$ and $i_d = -i_q$ under the assumption of constant inductances

In order to maximize the reluctant torque, the currents are assumed to respect the following equation:

$$i_d = -i_q. \tag{4}$$

These currents are assumed to be constant over one electrical period. The average value of the total torque over an electrical period is then independent of the variable part of e_d and e_q as shown on (5) where the symbol "$< \cdot >$" is used to express the average value over one electrical period.

$$\begin{aligned} < \Gamma_{em} > &= n_{pp}\frac{3}{2}(L_d - L_q)i_d i_q + \frac{3}{2\Omega}(< e_d > - < e_q >)i_d, \\ &= n_{pp}\frac{3}{2}\left[-(L_d - L_q)i_d^2 - \sqrt{3}e_0 sin(\delta_0 + \frac{\pi}{4})i_d\right]. \end{aligned} \tag{5}$$

From equation (5), it is clear that, provided that e_0 is large enough and i_d small enough, both δ_0 and the sign of i_d have an effect on the torque direction. The parameter δ_0 corresponds physically to the angle between the "d" axis of the rotor and its residual magnetism ϕ_f [14]. Four general value sets of δ_0 corresponding to the position of ϕ_f in the four sectors represented on Fig. 2 are considered. The Table 1 resumes the possible combinations. For each combination, the table explicitly expresses whether or not the EMF torque produced by the interaction of the residual magnetism and the current vector I_{rel} is beneficial to the voltage build-up.

Table 1 Overview of the impact of the EMF torque on the success of the voltage build-up

residual flux	$i_d > 0$ **&** $i_q < 0$	$i_d < 0$ **&** $i_q > 0$
sector 1	beneficial	non beneficial
sector 2	significantly beneficial	significantly non beneficial
sector 3	non beneficial	beneficial
sector 4	significantly non beneficial	significantly beneficial

The EMF torque is beneficial if it is of the same sign of the reluctant torque leading to a larger total torque, namely negative in this study case. The EMF torque is qualified as significantly beneficial when the angle between I_{rel} and ϕ_f is close to the optimum, namely $\frac{\pi}{2}$. On the opposite, the EMF torque is non beneficial, respectively significantly non beneficial, when it is of the opposite sign of the reluctant torque, respectively when the angle between I_{rel} and ϕ_f is close to its worst case, namely $-\frac{\pi}{2}$.

Thereby the direction of the residual flux is as much important as its amplitude for increasing the chances of success of a voltage build-up procedure for the SynRG. Indeed, even if the amplitude of the residual magnetism is large, if its direction is not advantageous, the voltage build-up is not significantly facilitated. Even worse, for a large residual magnetism, say in sector 2, if the current direction is not wisely chosen, considering $i_d < 0$, the EMF torque is significantly non beneficial. In this case, the larger the residual magnetism, the lower the chances of voltage build-up.

However, from the Table 1, it appears that for any residual magnetism direction, meaning any represented sector, the beneficial or significantly beneficial effect of the EMF torque is reachable by choosing wisely the sign of i_d via the control algorithm. Moreover, if the residual magnetism direction is selectable, it is desirable to place it in the sectors 2 or 4 and to choose the sign of i_d in adequacy so as to produce a significantly beneficial EMF torque.

The Fig. 2 illustrates the previous explanations where the current i_d is negative and the direction of the residual magnetism is $\delta_0 = -\frac{3\pi}{4}$. In this conditions the EMF torque is significantly beneficial to the voltage build-up. Indeed, the interaction between ϕ_f and I_{rel} produces a negative torque as defined as Γ_{em}. Moreover, the angle between ϕ_f and I_{rel} being $\frac{\pi}{2}$, the EMF torque is maximized.

4 Proposed procedure for the voltage build-up

4.1 Magnetization procedure

In a preliminary stage, the machine is magnetized in the desired direction via a magnetization procedure.

The machine is demagnetized by generating a decreasing rotating flux in stand-still conditions. From there, it can be magnetized in a chosen direction $\delta_0^{\#}$ in the rotor reference frame. By increasing the current in the direction $\delta_0^{\#}$,

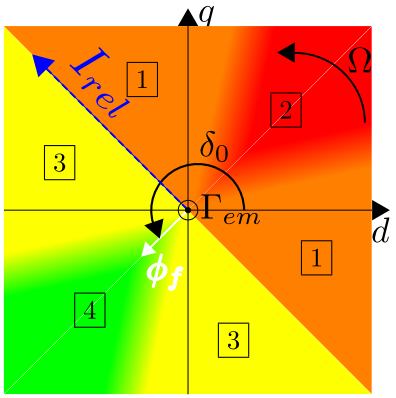

Fig. 2 Schematic representation of the effect of the residual magnetism direction on the voltage build-up when $i_d = -i_q < 0$

the magnetization follows the initial magnetization curve. Once the desired current is reached, we reduce the current down to zero. At this point, the magnetism is non-zero because of the magnetic hysteresis. It is known that the "d" axis is more likely to be magnetized that the "q" axis because of its greater amount of iron. This results in a larger residual magnetism in the "d" direction, leading to a direction of magnetization δ_0 possibly slightly different from $\delta_0^{\#}$. To overcome this issue, during the proposed procedure, the back EMF are estimated on-line in order to obtain the actual value of δ_0. The magnetization procedure is more detailed in [14].

Remark 2 For a real implemented system, it is desirable to perform this magnetization procedure before shutting down the power recovery. Thereby, the next voltage build-up is facilitated.

4.2 Controlled voltage build-up of the SynRG

During a first phase, the converter is uncontrolled. Its behaviour is similar to a three-phase diode rectifier. At the considered speed and magnetization, the back EMF are to low to make the diodes conductive. During this first phase, the DC voltage stays close to zero and does not increase significantly.

Secondly, the machine is short circuited via the controlled converter. This operation is possible because the DC voltage is quasi zero and the back EMF are low. During this second phase, the SynRG's back EMF are deduced from a short-circuit measurement and the knowledge of the machine's parameters. Thus their directions and magnitudes are verified. The on-line back EMF estimation method is detailed by the authors in [13].

In a third phase, smooth current references ramps respecting $i_d = -i_q$ are generated. During this phase, the system operates in a saturation zone. Indeed, the DC voltage is low, and the duty cycles are large, then close to their limits. The current references are given to field oriented current controllers with anti-wind-up loops. The slopes values are chosen small enough so as they can be followed even if the system operates close to the saturation zone.

Table 2 Main Parameters of the Synchronous Reluctance Machine

Parameters	Value	Units
Base speed (mechanical) Ω	1500	*rpm*
Number of pole pairs n_{pp}	2	–
Rated current I_n	4.5	*A*
Power P_n	1500	*W*
Nominal phase voltage V_n	230	*V*
Resistance per phase R_s	2.6	Ω
Unsaturated d-axis inductance L_d	0.289	*H*
Unsaturated q-axis inductance L_q	0.095	*H*

Remark 3 This procedure is parametrized by the choice of $\delta_0^{\#}$ in the preliminary stage and the choice of the sign of i_d in the last phase. By choosing a coherent combination of these parameters based on the Table 1, the chances of success of the voltage build-up can be notably increased.

Finally, when the DC voltage is large enough, the control saturations are no more an issue and the references slope can eventually be steeped. Afterwards a voltage control loop may be activated ensuring a robust voltage regulation regarding speed or load changes.

5 Experimental results

5.1 Description of the test bench

The system represented on Fig. 1 is implemented. For the experimental tests, a BSR90LE154055FB5 SynRM from Bonfiglioli is used. Its main characteristics are listed in Table 2. A Leroy-Somer 95UMC300HAAAA Permanent Magnet Synchronous Machine (PMSM) with the same speed and power range is attached to the SynRG by the shafts. This PMSM is used as a prime mover to drive the SynRG at a constant speed. The PMSM is fed through three-phase inverters composed of NTHL080N120SC1 SiC MOSFET. The same type of transistors are used for the active rectifier connected to the SynRG. The main benefit of this technology for the considered operation is to minimize the voltage drops at the switches terminals. The position and speed measurements are provided by an incremental encoder with 5000 points per mechanical revolution. All acquisitions are extracted through a dSpace MicroLabBox Rapid Control Prototyping (RCP) System. Two capacitors of 3300 μF are connected in series on the DC side of the power converter. A resistor R_L^0 of 11 kΩ is connected as a safety load at the capacitors terminals.

5.2 Verification of the average torque analysis

The first experimental test corresponds to a situation where the EMF torque is not beneficial to the voltage build-up.

The SynRG is firstly magnetized with a desired residual magnetism direction $\delta_0^{\#} = \frac{3}{4}\pi = 2.3562$ rad. The amplitude

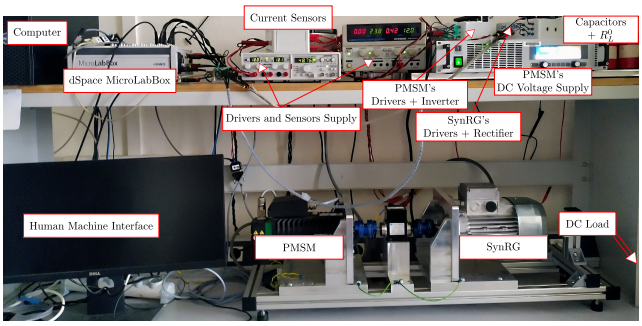

Fig. 3 Experimental test bench

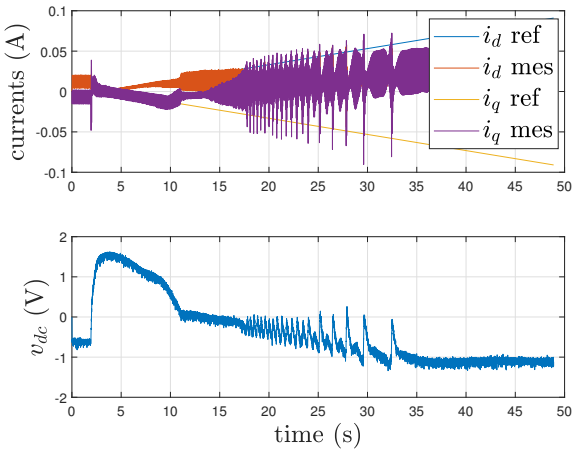

Fig. 4 Voltage build-up attempt in a non beneficial situation

of the magnetizing current is $I_0 = 1.41$ A. Afterwards, the PMSM drives the SynRG at a constant and positive speed $\Omega = 500$ rpm. After the uncontrolled phase, the back EMF are estimated as $< e_d >= -0.1$ V and $< e_q >= -0.34$ V. From there, the actual residual magnetism direction is determined as $\delta_0 = 2.8556$ rad corresponding to the sector $\boxed{3}$ in the Table 1 and on Fig. 2. The actual residual magnetism direction δ_0 is slightly bigger than $\delta_0^{\#}$. This is coherent with the fact that the direct direction is more likely to be magnetized. Then a constant slope respecting $i_d = -i_q > 0$ are generated for the current references. The slope is $0.002A/s$ and the initial current references are zeros. The results of this first experiment are shown on Fig. 4. After a short EMF estimation phase, the two currents follow their references until about $t = 10s$. During this phase, although the reluctant torque is negative, the voltage decreases. This is explained by the preponderance of the EMF torque at low current. The EMF torque is positive, leading to a motor operation of the machine and thus an impossibility of voltage build-up. After $t = 10s$ the voltage is too low and the currents do not follow their references anymore. The system is then uncontrolled and its behaviour is obviously not desirable. As predicted by the Table 1, the EMF torque is non beneficial and then the voltage build-up fails in the conditions of this first experiment.

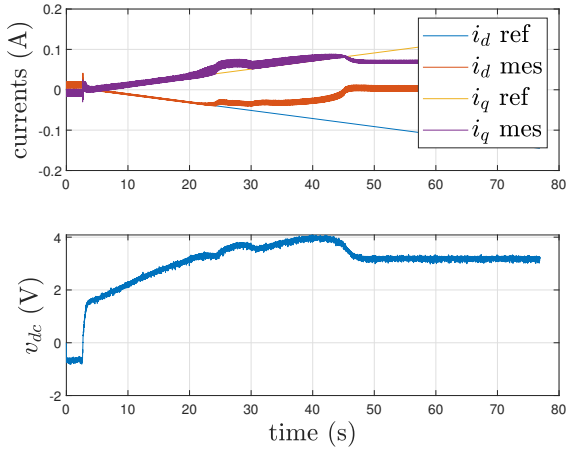

Fig. 5 Voltage build-up attempt in a beneficial situation

In a second experiment, a beneficial situation is tested The procedure is applied with $\delta_0^{\#} = \frac{3}{4}\pi = 2.3562$ rad ($\delta_0 = 2.8556$ rad corresponding to the same sector $\boxed{3}$ as before) and $i_d < 0$.

The very same magnetization procedure as before has been applied and only the i_d and i_q directions have changed. The results are shown on Fig. 5. The DC voltage evolution is quite different and more desirable than in the first experiment. After a short EMF estimation phase, the two currents follow their references until about $t = 23s$. During this phase, the DC voltage increases as wanted. Indeed, not only the reluctant torque but also the EMF torque are negative, leading to a larger negative total torque. However, the currents finally fail to follow their references. Again, from that moment, the system is completely saturated (the duty cycles reach their limits) and it is not normally controlled anymore. Finally the DC voltage drops and is not expected to increase, the experiment is stopped. In this second experiment, the voltage build-up fails too. The situation was beneficial but not enough to ensure a complete voltage build-up.

5.3 Validation of the proposed strategy

In a third experiment, the parameters are chosen so as to produce an EMF torque significantly beneficial to the voltage build-up. In practice, these parameters are chosen as $\delta_0^{\#} = -3/4\pi = -2.3562$ rad and $i_d < 0$.

The machine is firstly magnetized in the selected direction and under the same magnetizing current amplitude as before, namely $I_0 = 1.41$ A. The PMSM drives the SynRG at a constant and positive speed $\Omega = 500$ rpm. The back EMF estimation leads to $< e_d >= 0.1$ V and $< e_q >= -0.34$ V. From there, the actual back EMF direction is determined as $\delta_0 = -2.8556$ rad corresponding to the sector $\boxed{4}$ on Fig. 2. The currents references respecting $i_d = -i_q < 0$ are generated. The results are given on Fig. 6. Here the currents follow their references during all the experiment. The DC voltage

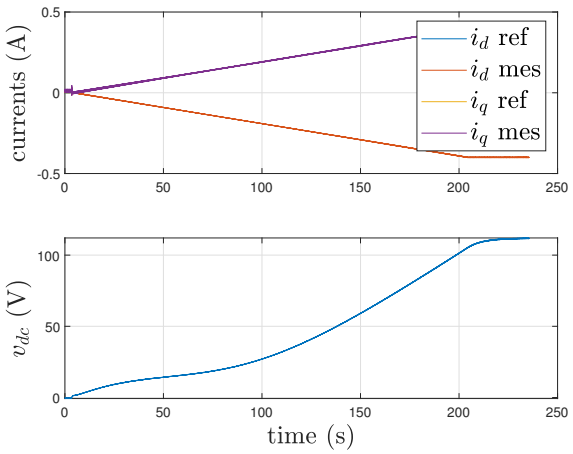

Fig. 6 Voltage build-up attempt in a significantly beneficial situation

continuously increases and the system is controlled at any time. The voltage build-up succeeded.

6 Conclusion

The interaction between the residual magnetism within the rotor of the SynRG and its currents produces a torque that can either be helpful or harmful for the voltage build-up. Thus, in addition with the commonly known minimum amplitude of the residual magnetism requested, this paper shows that the direction of this magnetization has a tremendous importance for achieving a successful voltage build-up of a SynRG. However, the worst cases, namely cases where the residual magnetism and the reluctance of the machine are antagonist, are preventable with the control algorithm by choosing the sign of i_d and i_q. The proposed procedure with the wisely chosen parameters, including the beforehand choice of the magnetization direction, ensures the voltage build-up of the generator even at a reduced speed of one third of the nominal. As a perspective, the procedure and the control can be improved to make the voltage build-up faster. This would make it suitable for regenerative or dynamic post-failure safety braking in electric traction applications.

References

1. Branko Ban, Stjepan Stipetić, and Mario Klanac. Synchronous reluctance machines: Theory, design and the potential u se in traction applications. In *2019 International Conference on Electrical Drives & Power Electronics (EDPE)*, pages 177–188. IEEE, 2019.
2. A. Boglietti and M. Pastorelli. Induction and synchronous reluctance motors comparison. In *2008 34th Annual Conference of IEEE Industrial Electronics*, pages 2041–2044, 2008.
3. Ion Boldea, Lucian N Tutelea, Leila Parsa, and David Dorrell. Automotive electric propulsion systems with reduced or no permanent magnets: An overview. *IEEE Transactions on Industrial Electronics*, 61(10):5696–5711, 2014.
4. JM Elder, JT Boys, and JL Woodward. The process of self excitation in induction generators. In *IEE Proceedings B (Electric Power Applications)*, volume 130, pages 103–108. IET, 1983.
5. S Hazra and P Sensarma. Vector approach for self-excitation and control of induction machine in stand-alone wind power generation. *IET Renewable Power Generation*, 5(5):397–405, 2011.
6. S Hazra and PS Sensarma. Self-excitation and control of an induction generator in a stand-alone wind energy conversion system. *IET renewable power generation*, 4(4):383–393, 2010.
7. Maged Ibrahim and Pragasen Pillay. The loss of self-excitation capability in stand-alone synchronous reluctance generators. *IEEE Transactions on Industry Applications*, 54(6):6290–6298, 2018.
8. Thomas Jahns. Getting rare-earth magnets out of ev traction machines: A review of the many approaches being pursued to minimize or eliminate rare-earth magnets from future ev drivetrains. *IEEE Electrification Magazine*, 5(1):6–18, 2017.
9. Subramaniam Senthil Kumar, Natarajan Kumaresan, Muthiah Subbiah, and Mahendhar Rageeru. Modelling, analysis and control of stand-alone self-excited induction generator-pulse width modulation rectifier systems feeding constant dc voltage applications. *IET Generation, Transmission & Distribution*, 8(6):1140–1155, 2014.
10. Seyede Sara Maroufian and Pragasen Pillay. Self-excitation criteria of the synchronous reluctance generator in stand-alone mode of operation. *IEEE Transactions on Industry Applications*, 54(2):1245–1253, 2017.
11. Mauro Di Nardo, Giovanni Lo Calzo, Michael Galea, and Chris Gerada. Design optimization of a high-speed synchronous reluctance machine. *IEEE Transactions on Industry Applications*, 54(1):233–243, 2018.
12. Anton Rassolkin, Hamidreza Heidari, Ants Kallaste, Toomas Vaimann, Jaime Pando Acedo, and Enrique Romero-Cadaval. Efficiency map comparison of induction and synchronous reluctance motors. In *2019 26th International Workshop on Electric Drives: Improvement in Efficiency of Electric Drives (IWED)*, pages 1–4. IEEE, 2019.
13. Laurent Schuller, Romain Delpoux, Jean-Yves Gauthier, and Xavier Brun. Online estimation and compensation of back-electromotive forces for synchronous reluctance machine. In *IECON 2021–47th Annual Conference of the IEEE Industrial Electronics Society*, pages 1–6. IEEE, 2021.
14. Laurent Schuller, Jean-Yves Gauthier, Romain Delpoux, and Xavier Brun. Dynamical model of residual magnetism for synchronous reluctance machine control. *IEEE Transactions on Industrial Electronics*, pages 1–1, 2021.
15. Alireza Siadatan, Mehdi Kholousi Adab, and H Kashian. Compare motors of toyota prius and synchronous reluctance for using in electric vehicle and hybrid electric vehicle. In *2017 IEEE Electrical Power and Energy Conference (EPEC)*, pages 1–6. IEEE, 2017.
16. G.K. Singh. Self-excited induction generator research—a survey. *Electric Power Systems Research*, 69(2):107–114, 2004.
17. A. Vagati, G. Franceschini, I. Marongiu, and G.P. Troglia. Design criteria of high performance synchronous reluctance motors. In *Conference Record of the 1992 IEEE Industry Applications Society Annual Meeting*, pages 66–73 vol.1, 1992.
18. Yawei Wang, Nicola Bianchi, Silverio Bolognani, and Luigi Alberti. Synchronous motors for traction applications. In *2017 International Conference of Electrical and Electronic Technologies for Automotive*, pages 1–8. IEEE, 2017.
19. Kai Zhang, Zhenyu Shan, and Juri Jatskevich. Estimating switching loss and core loss in dual active bridge dc-dc converters. In *2015 IEEE 16th Workshop on Control and Modeling for Power Electronics (COMPEL)*, pages 1–6, 2015.